

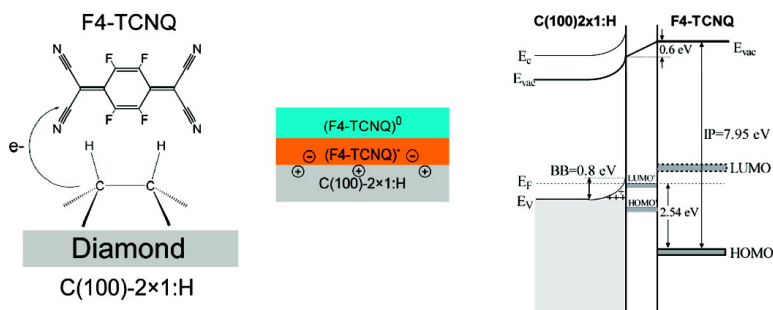
Communication

Surface Transfer Doping of Diamond (100) by Tetrafluoro-tetracyanoquinodimethane

Dongchen Qi, Wei Chen, Xingyu Gao, Li Wang, Shi Chen, Kian Ping Loh, and Andrew T. S. Wee

J. Am. Chem. Soc., **2007**, 129 (26), 8084-8085 • DOI: 10.1021/ja072133r • Publication Date (Web): 12 June 2007

Downloaded from <http://pubs.acs.org> on May 18, 2009



More About This Article

Additional resources and features associated with this article are available within the HTML version:

- Supporting Information
- Links to the 4 articles that cite this article, as of the time of this article download
- Access to high resolution figures
- Links to articles and content related to this article
- Copyright permission to reproduce figures and/or text from this article

[View the Full Text HTML](#)



ACS Publications
High quality. High impact.

Surface Transfer Doping of Diamond (100) by Tetrafluoro-tetracyanoquinodimethane

Dongchen Qi,[†] Wei Chen,[†] Xingyu Gao,^{*,†} Li Wang,[†] Shi Chen,[†] Kian Ping Loh,[‡] and Andrew T. S. Wee^{*,†}*Department of Physics, National University of Singapore, 2 Science Drive 3, Singapore 117542, and Department of Chemistry, National University of Singapore, 3 Science Drive 3, Singapore 117543*

Received March 27, 2007; E-mail: phygaoyx@nus.edu.sg; phyweets@nus.edu.sg

Doping of semiconductors is conventionally achieved by incorporating dopants into the host semiconductor lattice. Recently, a novel p-type surface transfer doping by transferring electrons from a semiconductor to surface “dopants” has been proposed for the fabrication of nanoscale planar doped electronic devices.^{1–6} On hydrogenated diamond, the surface transfer doping model was used to explain the occurrence of high surface conductivity when diamond is exposed to atmosphere⁶ or deposited with fullerenes.^{1–2} However, no direct measurement of charge transfer between diamond and its surface adsorbates has been reported so far. In addition, characterizations of electronic structures at the interface, which are crucial for both fundamental understanding and device application, are still lacking. Here, we unambiguously demonstrate p-type surface transfer doping of hydrogenated diamond (100) by the molecular electron acceptor, tetrafluoro-tetracyanoquinodimethane (F4-TCNQ). The interface electronic structure and energy level alignment are also determined.

It is well-known that the negative electron affinity of hydrogenated diamond leads, in spite of its large band gap (5.47 eV), to an exceptionally low ionization potential (IP).⁷ Because of its strong electron accepting nature (reported electron affinity (EA) of 5.24 eV),⁸ F4-TCNQ is widely used for controlled p doping in hole transporting organic layers^{8–11} or as an optimizer to tune the hole-injection barrier at organic–metal interfaces.¹² Therefore, F4-TCNQ on diamond is an excellent test bed to examine surface transfer doping, since the diamond valence band maximum (VBM) lies above the lowest unoccupied state (LUMO) of F4-TCNQ, thereby favoring electron transfer from diamond to F4-TCNQ molecules.

The charge transfer at the F4-TCNQ/diamond interface was monitored by synchrotron-based photoemission spectroscopy (PES). Details of the sample preparation and experimental setup can be found in the Supporting Information. PES spectra of N 1s evolution with increasing nominal thickness of F4-TCNQ is shown in Figure 1a. Initial deposition up to 0.5 Å leads to the formation of a pronounced peak at 397.50 eV (N-1) and a broad component at higher binding energy (BE). At 1.0 Å nominal thickness, the higher BE peak (N-2, 398.90 eV) becomes stronger than N-1. Further deposition results in a continuous increase in N-2 peak intensity and a decrease of N-1. In comparison with F4-TCNQ on Au,¹² we assign the higher BE peak N-2 to neutral F4-TCNQ (in multilayers) and the lower BE peak N-1 to anion molecules in direct contact with diamond with their C≡N groups extracting electrons from diamond.^{13,14} Peak N-S centered at 2.60 eV higher BE than peak N-2 is attributed to shakeup processes.¹³ The loss of electrons (accumulation of holes) in the diamond surface region is further corroborated by the C 1s spectra shown in Figure 1b. A substantial shift (0.65 eV) of the diamond peak to lower BE is immediately

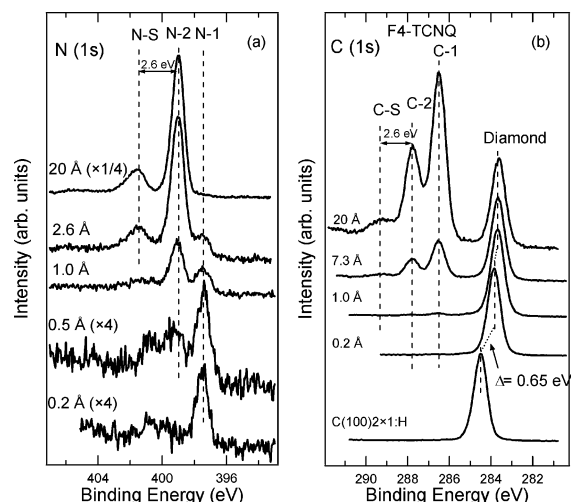


Figure 1. (a) N 1s XPS spectra (photon energy, 500 eV) and (b) C 1s XPS spectra (photon energy, 350 eV) of F4-TCNQ on diamond with increasing thickness. C 1s spectra are all normalized to the same diamond peak intensity for better viewing.

observed at the initial nominal thickness of 0.2 Å. This shift continues to increase with subsequent deposition and saturates at 0.80 eV at the nominal thickness of 1.0 Å. This indicates an upward band bending of 0.80 ± 0.05 eV at the diamond surface region, resulting from hole accumulation to balance the negatively charged anion molecules.¹⁵ Further deposition leads to virtually no change of the diamond peak position, and three new components (C-1, C-2, and C-S) related to carbon atoms in F4-TCNQ can be clearly resolved after several molecular layers are formed. C-S, similar to N-S, is also related to shakeup processes.¹³ The appearance of the anion F4-TCNQ interlayer species, together with the upward band bending inside diamond, clearly reveals electron transfer from diamond to surface acceptors, or p-type surface transfer doping.

Figure 2a shows the evolution of valence band spectra of hydrogenated diamond with increasing F4-TCNQ thickness. After the initial deposition of 0.2 Å, a rigid shift of 0.65 eV toward lower BE of the diamond features can be observed, consistent with that of the diamond C 1s peak (Figure 1b) and thus is attributed to the upward band bending. Further deposition leads to an overall attenuation of the diamond features and the emergence of several new features originating from F4-TCNQ at the higher BE region. At the nominal thickness of 11.4 Å, various orbitals of F4-TCNQ can be clearly resolved, with the highest occupied molecular orbital (HOMO) peak at 3.20 ± 0.05 eV and its edge at 2.54 ± 0.05 eV, consistent with previous measurements of F4-TCNQ on Au.⁸ After deposition of 0.5 Å, a close-up of the region near the Fermi level in Figure 2b reveals additional shoulders centered at around 0.4 and 1.4 eV and clearly seen in the difference spectrum after

[†] Department of Physics.[‡] Department of Chemistry.

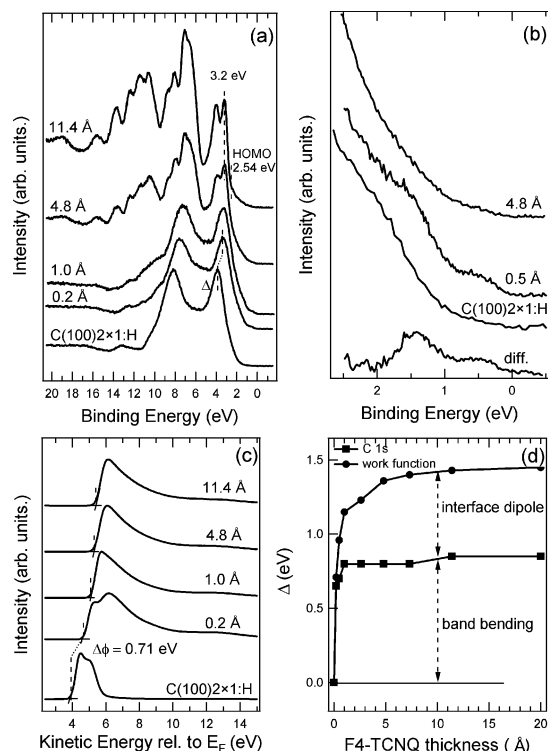


Figure 2. (a) UPS spectra (photon energy, 60 eV) of pristine hydrogenated diamond and after F4-TCNQ deposition of increasing thickness; (b) near the E_F region of the UPS spectra; (c) secondary electron cutoff of hydrogenated diamond with increasing F4-TCNQ thickness, indicating the work function change; (d) diamond C 1s peak shift and work function change as function of F4-TCNQ thickness.

subtracting the diamond contribution (bottom spectrum in Figure 2b). These two gap states were previously observed when F4-TCNQ formed a charge-transfer complex on a Au surface¹² and were attributed to the relaxed HOMO (higher BE) and partially filled LUMO (lower BE) of the anion molecules, respectively.^{16,17} The intensity of these two peaks is reduced after the deposition of multilayers (top spectrum in Figure 2b), where molecules are in their neutral state.

Another consequence of the charge transfer at the interface is the formation of an interface dipole,¹⁸ which is indicated by the sudden increase of work function after initial deposition of 0.2 Å as shown in Figure 2c. However, it should be noted that the increase in work function after F4-TCNQ deposition should also incorporate contribution from the band bending in the diamond surface. To separate the interface dipole contribution, the increase in work function is plotted together with the shift of the diamond C 1s peak as a function of F4-TCNQ nominal thickness (Figure 2d). Throughout the deposition, the change of work function is substantially larger than the C 1s shift of the diamond peak, and the difference between them gradually enlarges with increasing thickness and reaches a maximum of 0.6 eV, which is due to the interface dipole.

With the knowledge of the electronic structures at the F4-TCNQ/diamond interface, we are now able to sketch the energy level alignment diagram before (Figure 3a) and after F4-TCNQ deposition (Figure 3b). Once the contact is formed, electrons flow from the diamond valence band to the F4-TCNQ side until equilibrium is reached (Figure 3b). This surface transfer doping process is so efficient that the diamond VBM is moved 0.2 eV above the Fermi level at the diamond surface region. According to Poisson's equation and Fermi statistics (see Supporting Information for calculation details),³ the hole areal density in diamond can be estimated to be about $1.6 \times 10^{13} \text{ cm}^{-2}$, which is substantially larger than the

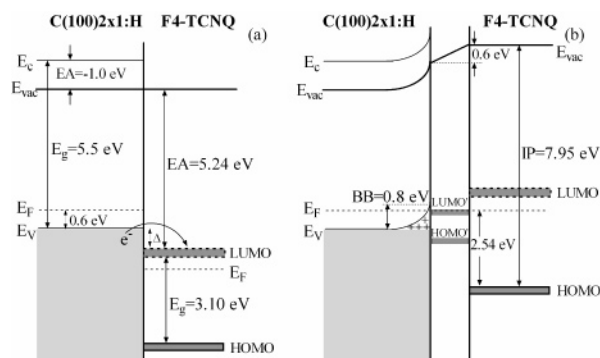


Figure 3. Energy level diagram of (a) before deposition of F4-TCNQ, E_g and EA of F4-TCNQ are taken from ref 8 and (b) after deposition of F4-TCNQ (20 Å). LUMO' and HOMO' are the two gap states of the anion F4-TCNQ molecules at the interface. The position of LUMO is obtained by adding a band gap of 3.10 eV to the HOMO position. Determination of diamond's E_V position, NEA, and the IP of F4-TCNQ are described in Supporting Information.

intrinsic boron doping level of the diamond sample (around 10^{10} cm^{-2}), and is comparable to maximum hole density achieved by Strobel et al. using $\text{C}_{60}\text{F}_{48}$.²

In conclusion, we have unambiguously demonstrated a controllable surface transfer doping of hydrogenated diamond by the adsorption of F4-TCNQ molecules. A high areal density of holes in diamond of about $1.6 \times 10^{13} \text{ cm}^{-2}$ is formed. The results give us a better understanding of the electronic structure changes at the interface owing to surface transfer doping. This will pave the way for better selection of organic molecular acceptors to control the surface conductivity of semiconductors.

Acknowledgment. The authors gratefully acknowledge the support from National University of Singapore under the Grant No. R-144-000-107-112 and R-144-000-106-305.

Supporting Information Available: Experimental section, energy level determination, and areal hole density calculation. This material is available free of charge via the Internet at <http://pubs.acs.org>.

References

- (1) Strobel, P.; Riedel, M.; Ristein, J.; Ley, L. *Nature* **2004**, *430*, 439–441.
- (2) Strobel, P.; Riedel, M.; Ristein, J.; Ley, L.; Boltalina, O. *Diamond Relat. Mater.* **2005**, *14*, 451–458.
- (3) Ristein, J. *J. Phys. D: Appl. Phys.* **2006**, *39*, R71–R81.
- (4) Ristein, J. *Science* **2006**, *313*, 1057–1058.
- (5) Zhang, P. P.; Tevaarwerk, E.; Park, B. N.; Savage, D. E.; Celler, G. K.; Knezevich, I.; Evans, P. G.; Eriksson, M. A.; Lagally, M. G. *Nature* **2006**, *439*, 703–706.
- (6) Maier, F.; Riedel, M.; Mantel, B.; Ristein, J.; Ley, L. *Phys. Rev. Lett.* **2000**, *85*, 3472–3475.
- (7) Maier, F.; Ristein, J.; Ley, L. *Phys. Rev. B* **2001**, *64*, 165411.
- (8) Gao, W. Y.; Kahn, A. *Org. Electron.* **2002**, *3*, 53–63.
- (9) Blochwitz, J.; Pfeiffer, M.; Fritz, T.; Leo, K. *Appl. Phys. Lett.* **1998**, *73*, 729–731.
- (10) Zhou, X.; Pfeiffer, M.; Blochwitz, J.; Werner, A.; Nollau, A.; Fritz, T.; Leo, K. *Appl. Phys. Lett.* **2001**, *78*, 410–412.
- (11) Takenobu, T.; Kanbara, T.; Akima, N.; Takahashi, T.; Shiraishi, M.; Tsukagoshi, K.; Kataura, H.; Aoyagi, Y.; Iwasa, Y. *Adv. Mater.* **2005**, *17*, 2430–.
- (12) Koch, N.; Duhm, S.; Rabe, J. P.; Vollmer, A.; Johnson, R. L. *Phys. Rev. Lett.* **2005**, *95*, 4.
- (13) Lindqvist, J. M.; Hemminger, J. C. *J. Phys. Chem.* **1988**, *92*, 1394–1396.
- (14) Rojas, C.; Caro, J.; Grioni, M.; Fraxedas, J. *Surf. Sci.* **2001**, *482*, 546–551.
- (15) Takeuchi, D.; Riedel, M.; Ristein, J.; Ley, L. *Phys. Rev. B* **2003**, *68*, 041304.
- (16) Salaneck, W. R.; Friend, R. H.; Bredas, J. L. *Phys. Rep.* **1999**, *319*, 231–251.
- (17) Koch, N.; Rajagopal, A.; Ghijsen, J.; Johnson, R. L.; Leising, G.; Pireaux, J. J. *J. Phys. Chem. B* **2000**, *104*, 1434–1438.
- (18) Ishii, H.; Sugiyama, K.; Ito, E.; Seki, K. *Adv. Mater.* **1999**, *11*, 605–625.

JA072133R